

HIGH SPEED SWITCHING FOR
INTEGRATED OPTICAL APPLICATIONS

P.E. Jessop and B.K. Garside

Department of Engineering Physics
McMaster University
Hamilton Ontario



engineering
physics

McMaster University
Hamilton, Ontario, Canada

IC

P
91
C654
J47
1986

HIGH SPEED SWITCHING FOR
INTEGRATED OPTICAL APPLICATIONS

D.E. Jessop and B.K. Garside

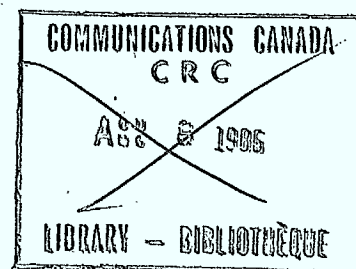
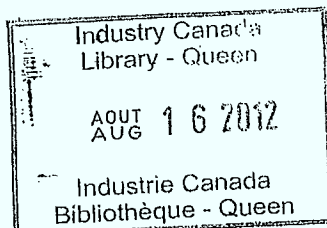
Department of Engineering Physics
McMaster University
Hamilton Ontario

Final Report

Department of Communications

Contract No. OST85 - 00241

July 1986



891
OK
JAP
1986

RECEIVED - 1986

RECEIVED - 1986

ORIGINAL DOCUMENT REVIEW AND PUBLICATION RECORD

SECTOR DGRC	BRANCH MOC	DATE August 1986
----------------	---------------	---------------------

PURPOSE This form is for use during review of the DOC-CR contractor reports.
It is designed to: record decisions for classification,
record reasons for classification and cautionary marking
provide for indexing requirements.

INSTRUCTIONS * 1 copy of the completed form must accompany the contractor report package submitted to the CRC Library.

* Complete the following items as applicable.

1. DOC-CR NO. DOC-CR-RC-86-004	2. DSS CONTRACT NO. 36100-5-0091
3. TITLE: High speed switching for integrated optical applications; final report	4. DATE July 1986
5. CONTRACTOR McMaster University	
6. SCIENTIFIC AUTHORITY K.O. Hill	7. LOCATION MOC/CRC
8. TEL. NO. 998-2720	
9. CONTRACTOR REPORT CLASSIFICATION: RELEASABLE <input checked="" type="checkbox"/> CONDITIONALLY RELEASABLE <input type="checkbox"/> NON-RELEASABLE <input type="checkbox"/>	

* REASONS FOR CLASSIFICATION:

10. NO. OF COPIES SUBMITTED TO LIBRARY:

EXECUTIVE SUMMARY ☐ FINAL REPORT ☒ 2 copies

1 copy rec'd 20/1/87

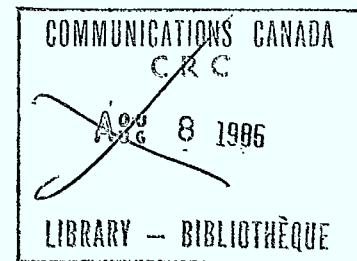
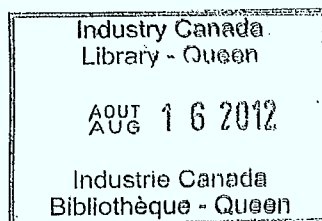
.....
Scientific Authority's Signature

.....
Date

This form is not official therefore it is not signed.

TABLE OF CONTENTS

Research Personnel	ii
Figure Captions	iii
1. Introduction	1
2. High Speed Interdigital Detectors	3
3. Thin Film Optical Waveguides	15
4. Integrated Optical Detectors	26
5. Conclusions	38
Appendix	40
References	42



RESEARCH PERSONNEL

Principal Investigators: Dr. P.E. Jessop
 Dr. B.K. Garside

Research Engineer: Dr. D.M. Bruce

Graduate Students: R.J. Seymour
 D. Cheong

Research Assistants: E.V. Bagi
 M.D. McPherson

ACKNOWLEDGEMENT

We gratefully acknowledge the assistance of Dr. C. K. Campbell in allowing us to make use of his mask making and mask alignment facilities.

FIGURE CAPTIONS

Page

1. Electrode pattern for small area interdigital photodetectors. 4
2. Measured and calculated response of the silicon-on-sapphire Schottky barrier detectors to a 40 psec (FWHM) laser pulse. 7
3. Relative responsivity of interdigital photoconductive detectors as a function of bias voltage. The detectors with aluminum electrodes had a higher sensitivity than those with gold electrodes. 10
4. Measured detector response to a 70 psec laser pulse. 11
Upper trace: photoconductive detector on p-type bulk Si.
Lower trace: photoconductive detector on Ge-on-GaAs.
5. Length of the visible stripes of light coupled into a ZnO waveguide as a function of substrate temperature during deposition. The longest stripe length had a measured attenuation of 9 dB/cm. 19
6. Scanning electron microscope photographs showing an edge-on view of a ZnO film. The SiO₂ buffer layer is visible between the film and the Si substrate. 21
7. Glass waveguide channel on an oxidized silicon substrate. A cleaved end surface of the wafer is shown at two different magnifications. 25
8. Upper trace: Mask Pattern #3 used to define the array of waveguide channels. 27
Lower trace: Mask pattern #2 used to define the 40 element detector array. 21 long electrodes are connected in common. There is a short electrode between each pair of long electrodes. The gap between electrodes is too narrow to be visible on this scale.
9. Upper trace: Expanded scale view of an individual element of mask #1, used to define regions of exposed silicon. 28
Lower trace: An individual detector element from mask #2.
10. Relative responsivity of a photoconductive detector as a function of the distance between the detector element and the illuminated spot on the silicon surface. The laser probe was mechanically chopped and was focussed to a diameter of 0.4 mm. 31

1. INTRODUCTION

High speed photodetectors are essential elements for optical communications, optoelectronic switching and integrated optical systems. For many applications there are advantages to a detector design which employs an interdigitated electrode geometry in which both contacts are on the top surface of a semiconductor. This geometry facilitates the monolithic integration of photodetectors with silicon or gallium arsenide electronic components and integrated circuit topologies [1]. It is also well suited to solving one of the most basic problems in integrated optics, that is the efficient coupling of the light from an optical waveguide channel into a photodetector which is co-fabricated on the same substrate [2]. The fabrication of such detectors is relatively simple when compared to p-i-n devices and can be used with a wide variety of materials. With interelectrode spacings reduced to several microns the carrier transit times are in the picosecond regime, thus making ultrafast detector response possible.

In this report we describe work which has been carried out over the past nine months. This work was aimed at developing new types of high speed photodetectors and techniques which can be used to incorporate these detectors into integrated optical device structures. Section 2 deals with the fabrication and characterization of discrete detector elements using an interdigitated electrode geometry to form either a photoconductor or a Schottky barrier detector. These devices were made using silicon-on-sapphire, silicon and germanium-on-gallium arsenide as the active materials. Section 3 describes an investigation of the use of rf sputtering for fabrication of thin film optical

waveguides and the formation of narrow waveguide channels using standard photolithographic techniques. The ability to make low loss waveguide channels is a necessary precondition to the longer term goal of developing integrated optical devices for high speed switching applications. In section 4 we describe an integrated photodetector which is similar to the discrete devices but has a different electrode configuration. As an integral part of its structure an optical waveguide channel is used to deliver an external optical signal to the small active area of the detector.

2. HIGH SPEED INTERDIGITAL DETECTORS

i) Schottky Barrier Devices

We have shown that a detector consisting of two sets of interlocked metal digits, forming back-to-back Schottky barriers on a semiconductor surface, is capable of efficient response on a time scale of tens of picoseconds [3,4]. By using semiconductor-on-insulator materials as substrates it is possible to reduce the depletion capacitance to very low levels. Then the device capacitance is dominated by the contribution from the interlocked digits, which can be less than 1 pF. Our detectors were fabricated on commercially obtained silicon-on-sapphire (SOS) films which were n-type, approximately 1 μm thick and had a nominal resistivity of 12 ohm-cm. The metal contact configuration is shown in Fig. 1. The detector active area was approximately 10^{-4} cm^2 . Gold was used for the contacts since it is known to form stable Schottky barriers on n-type silicon.

When a potential is applied between the two sets of digits, the negative contact becomes a reverse biased Schottky barrier while the positive contact is a forward biased barrier which behaves approximately as an ohmic contact. A depletion region will extend outward from the reversed biased digit for a distance that depends on the applied bias voltage and the silicon doping density. Electron-hole pairs which are generated by the incident light in this region are efficiently separated by the associated electric field with a response speed in the picosecond regime. In addition, there will also be electron hole pairs generated in the undepleted region of the surface where the electric field is quite small. These make a much weaker and slower contribution

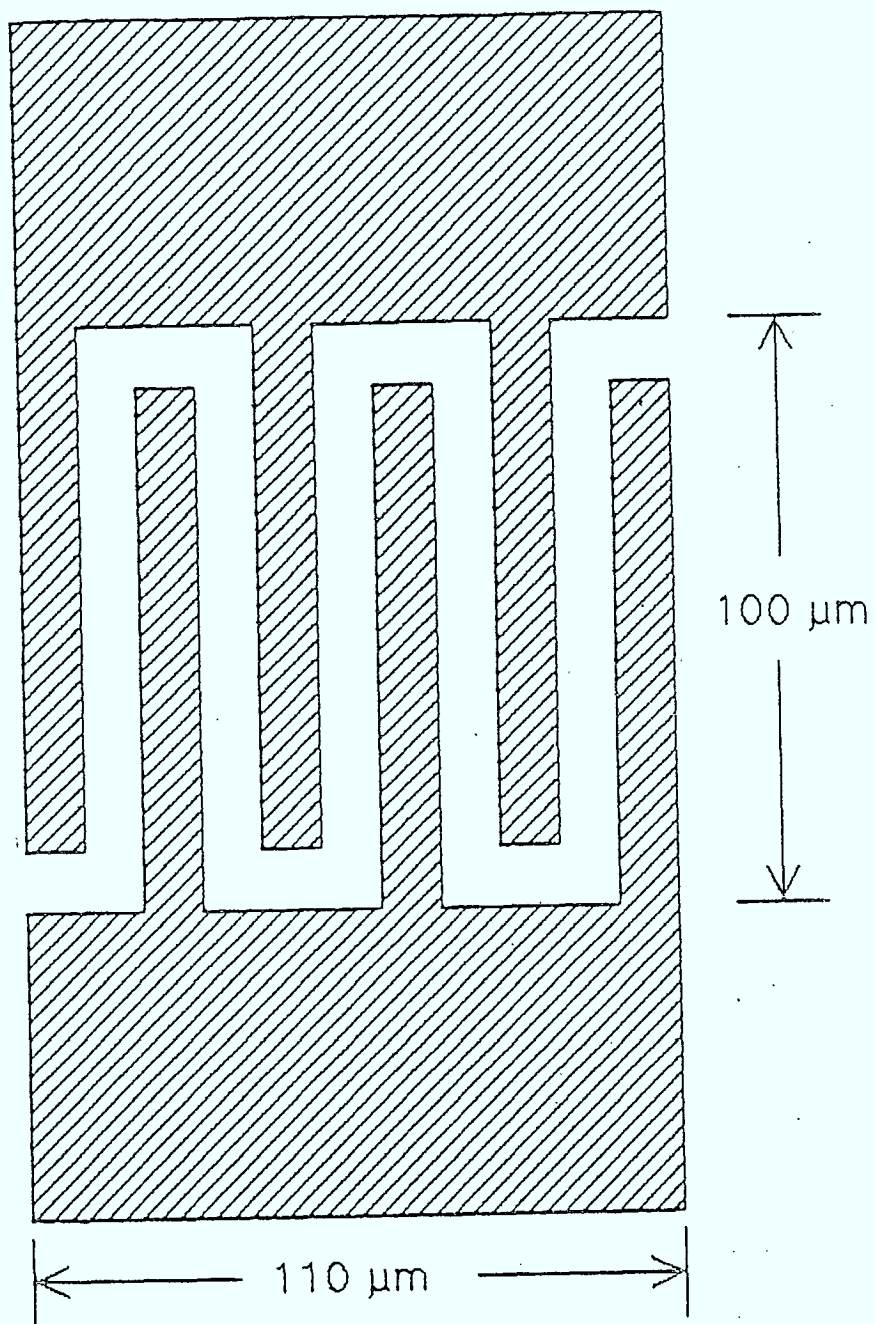


Figure 1

to the photocurrent since their collection relies on diffusion of the carriers within their carrier lifetime.

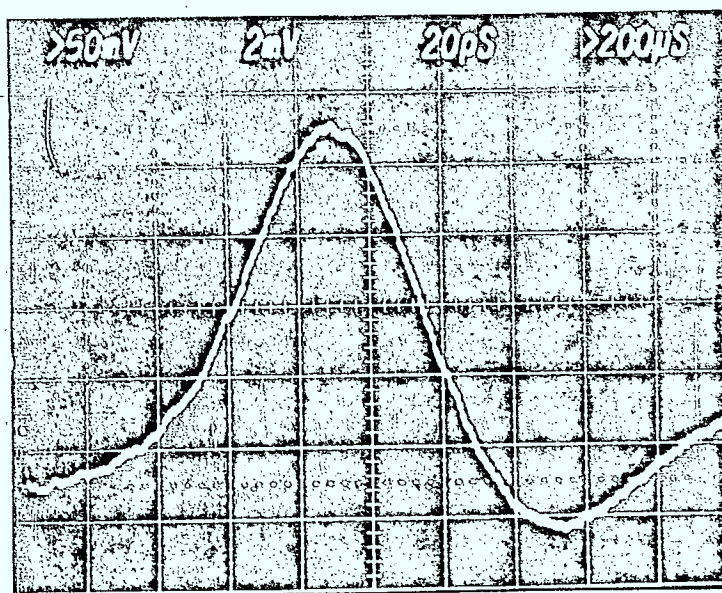
Both the steady state and the short pulse response characteristics of these detectors have been modelled by solving Poisson's equation, together with the carrier transport and continuity equations in two dimensions using a finite differences approach [5]. The predicted behaviour was in good agreement with results of a series of experimental measurements. In one of these a tightly focussed He-Ne laser beam (with a focal spot diameter of 1 to 2 μm) was scanned across the detector so that it was possible to observe separately the effects of illuminating either the depleted or undepleted region. Thus the width of the depleted region and the relative photoresponse of the two regions could be measured. From these measurements the silicon doping density and the carrier lifetime (approx. 400 psec) could be inferred. The former was in agreement with the known value for the substrate material and the latter was confirmed by subsequent observation of the response to pulsed illumination of the undepleted region alone. Fortunately, the response time of the detector, when it is illuminated uniformly over its entire area, is determined primarily by the collection of carriers that are generated in the depletion region. The theoretical model was used to predict the response to a Gaussian input pulse having a width (FWHM) of 40 psec. When convolved with the sampling oscilloscope's response function the predicted response time was 52 psec (FWHM), compared to an observed value of 46 ± 4 psec. Deconvolution of the detector response from the combined effects of

the input pulse width and the sampling oscilloscope response gives a response time of less than 30 psec. Fig. 2 shows the signal recorded on the sampling oscilloscope. These measurements were carried out using a fast pulsed AlGaAs laser at a wavelength of 900 nm. In a separate experiment, pulses from a mode locked dye laser at wavelengths of 616 nm and 308 nm (using frequency doubling) were also used and this confirmed that the detector response was less than 30 psec for illumination in the visible and ultraviolet as well.

Similar detectors were also fabricated by depositing interdigitated gold contacts directly onto the surface of bulk n-type silicon, rather than SOS. In this case the depletion depth was approximately 5 microns. Two major differences between the SOS and bulk silicon detectors are that in the latter the depletion capacitance is no longer insignificant and the carrier lifetime is much larger, which enhances the slow diffusion component of the photoresponse. Steady state probing of the spatial dependence of the detector response using the focussed He-Ne laser showed an almost uniform response over the entire region between the digits, not just from the depleted region as was the case for SOS substrates. Also, the pulsed response was on the order of 1 nsec long.

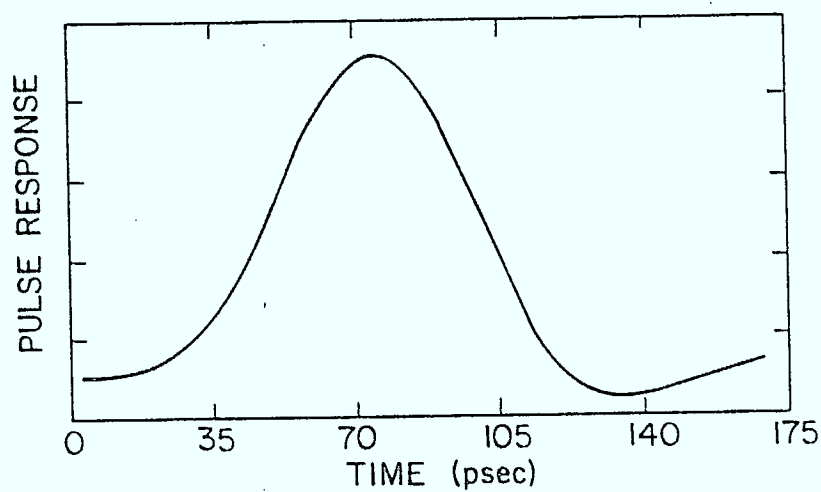
ii) Silicon Photoconductive Detectors

The same electrode configuration that was used for the Schottky barrier photodiodes also can be used to fabricate high speed photoconductive detectors. In this case the combination of semiconductor and electrode materials is such that ohmic rather than barrier contacts are formed. For optoelectronic



INCIDENT PULSE
40 PSEC FWHM

MEASURED RESPONSE



CALCULATED RESPONSE

Figure 2

switching applications [6] photoconductive detectors have the advantage that there is no charge accumulation or depletion layers as in the junction of a photodiode. Thus, the switching between the sensitive on-state and the insensitive off-state can be much faster. Also, photoconductors provide better isolation; that is, the sensitivity in the zero-bias "off" state is more nearly zero. Another advantage is that the detectors' responsivity can be enhanced by a certain amount of photoconductive gain. But since the gain is given by the ratio of the effective carrier lifetime to the carrier transit time between the electrodes, there is a tradeoff to be made between responsivity and response speed.

Several sets of detectors were fabricated by evaporating gold or aluminum contacts onto p-type silicon which had resistivity of either 10 or 1 ohm-cm. In the case of aluminum, post deposition heat treatment, consisting of ten minutes at 400°C, was used to ensure ohmic contacts. The I-V characteristics of the detectors (as measured on a curve-tracer) showed a resistance a few k Ω for the 10 ohm-cm silicon and about 100 Ω for the 1 ohm-cm silicon. This was consistent with the dark current that was observed to flow through a biased detector.

The detectors were mounted in a small gap that was made in a 50-ohm transmission line on a printed circuit board and the two electrodes were bonded to the opposite portions of the strip line. A DC bias voltage of 5V was connected to one side (through a 1 k Ω resistor) and the other side terminated in 50 Ω at a soldered-on rf connector. This mount had been previously used to

observe Schottky barrier detector response times on the order of 100 psec and so was quite adequate to measure the high frequency response of the photoconductive detectors.

First, the low frequency responsivity of these detectors was measured by recording the photocurrent generated by a mechanically chopped He-Ne laser beam. The diameter of the slightly focussed beam was larger than the detectors' active region. So the received optical power was taken to be the laser intensity (typically 1 mW/mm²) times the detector area (1.1×10^{-2} mm²). This is the total area of the interdigitated portion of the detector (excluding the large bonding pads), not just the open area between the contacts, which was about 55% of the total. The results ranged from 0.9 to 1.4 amps/watt for the 10 ohm-cm silicon devices and were about 0.06 amps/watt for the 1 ohm-cm devices. The variation of responsivity as a function of bias voltage is shown in Fig. 3.

The detectors' speeds of response were measured by observing the response to a 70 psec diode laser pulse on a sampling oscilloscope. For the modest bias voltages used, the carrier transit time between the electrodes is expected to be a few hundred psec. This is consistent with the observed risetime of the response but the long effective carrier lifetime of the 10 ohm-cm silicon resulted in fall times of 1-3 nsec as shown in Fig. 4. The devices with aluminum electrodes were about a factor of two faster than those with gold electrodes.

iii) Germanium-on-Gallium Arsenide

There is a fortuitous lattice constant match between Ge and GaAs which facilitates the epitaxial growth of Ge layers on GaAs

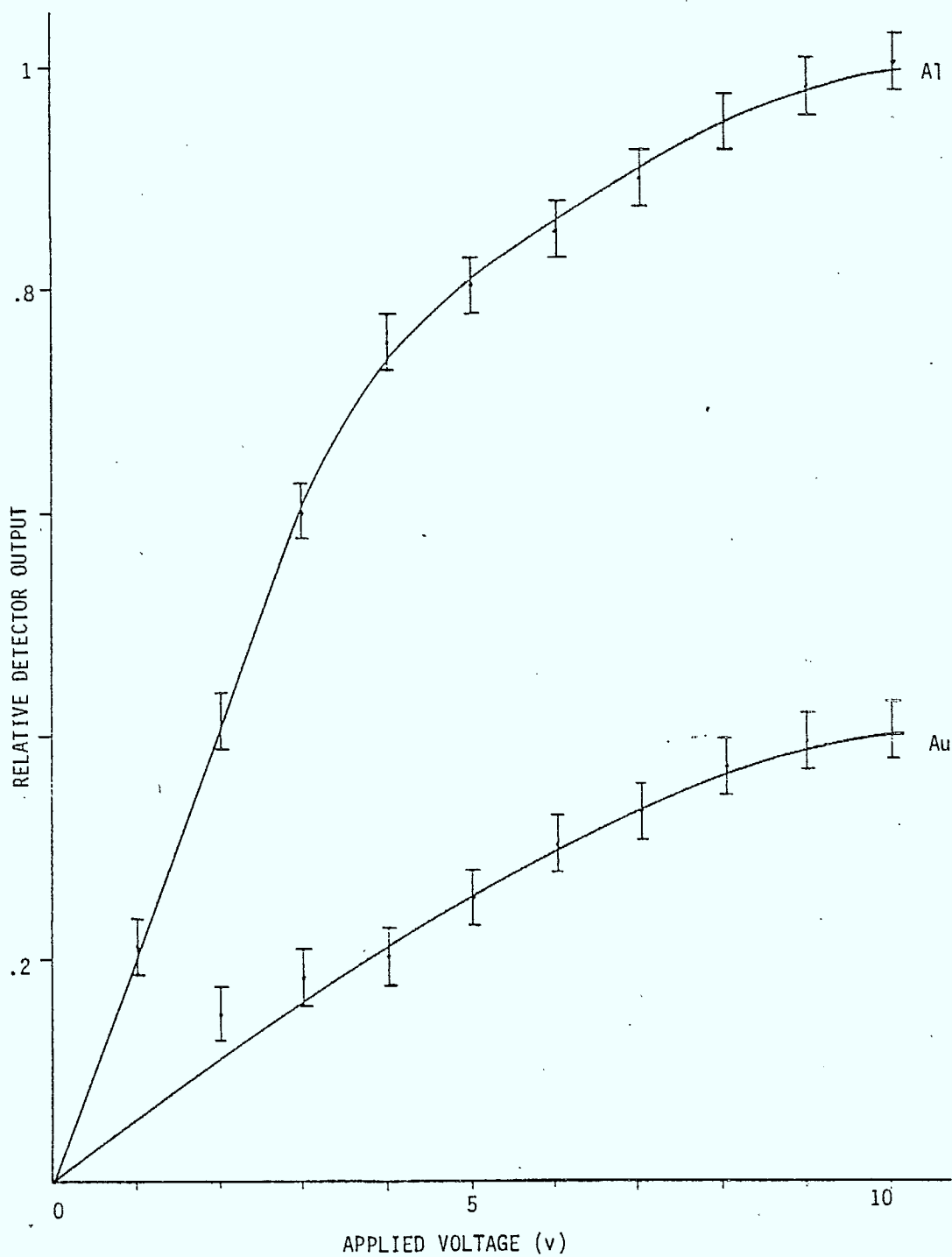
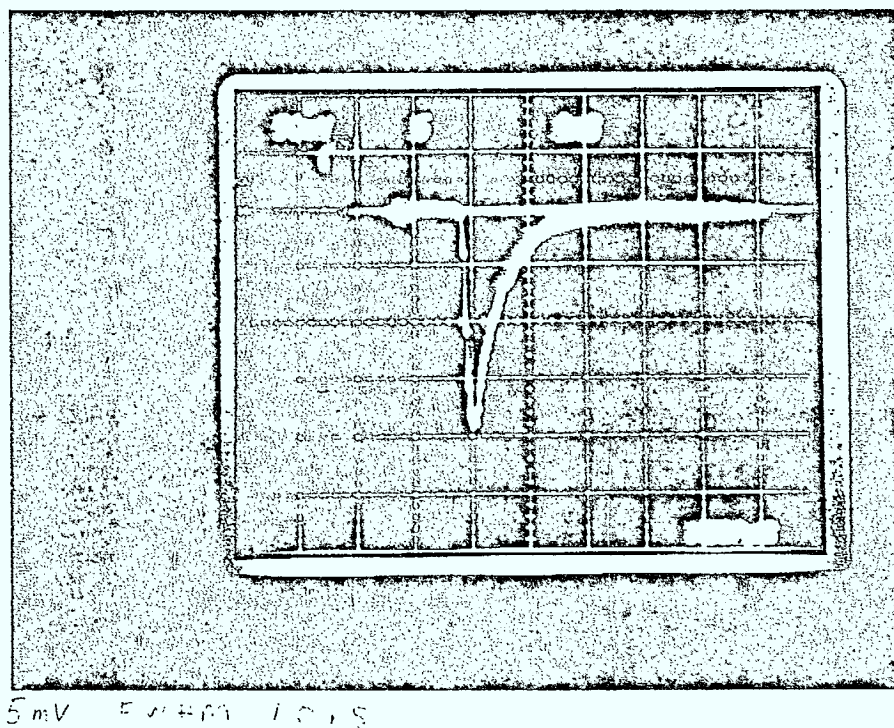


Figure 3



GPa: 1.

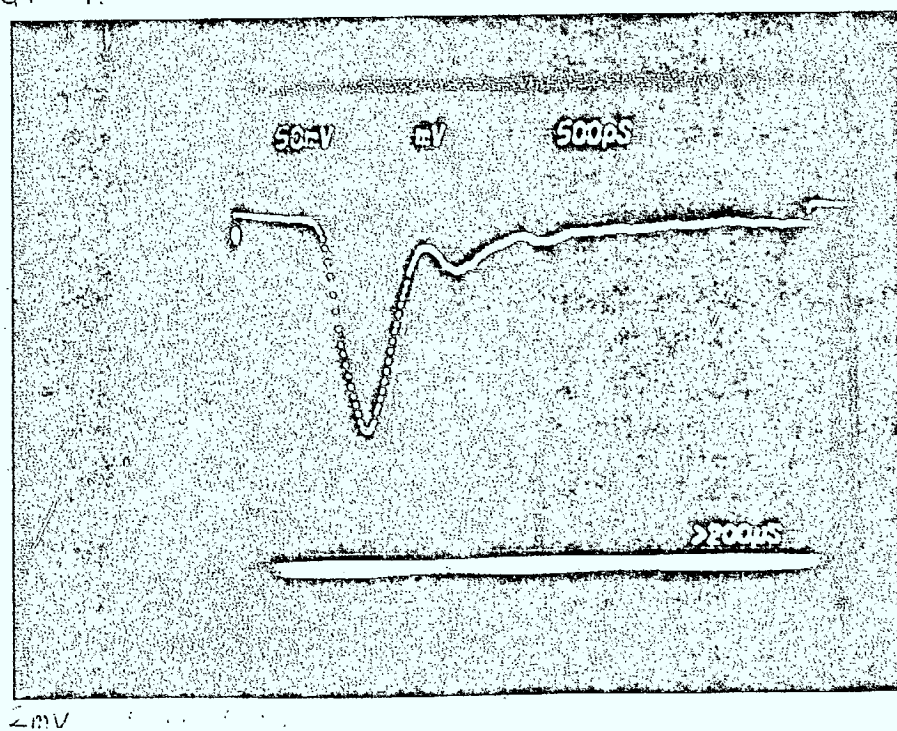


Figure 4

substrates. This has been demonstrated by many researchers employing sputtering [7], e-beam evaporation [8] and other techniques. This offers an interesting new material for photodetector fabrication since doped films on semi-insulating substrates would offer the same high speed advantages as the silicon-on-sapphire substrates. It is also an interesting system for integrated optics because ultimately one would prefer devices in which all of the components (sources, waveguides and detectors) were made from semiconductor epilayers. Ge-on-GaAs is an ideal combination for operation near the $1.3\text{ }\mu\text{m}$ wavelength region since GaAs is transparent (as a waveguide medium) and germanium is highly absorbing (for use as a detector). Ge-on-GaAs is also interesting for microelectronics, in general. There is currently a great deal of interest in growing GaAs on Si substrates. This is because of the potential advantages of combining devices using both of these semiconductors in a single integrated circuit. Much of the work has involved germanium intermediate layers in an attempt to accommodate the large lattice mismatch between GaAs and Si.

We have previously used rf sputtering to deposit crystalline films of Ge on GaAs and other substrates [9]. For the current project we had available a few p-type samples of Ge-on-GaAs films of varying carrier concentrations. Sputter deposition of additional films would have required the use of the sputtering system that was used for the waveguide deposition. This was impractical because of cross contamination concerns. Therefore, e-beam evaporation was also employed. A substrate heater was built

which could preheat the GaAs to 600°C in order to desorb the surface oxides. During deposition the substrate temperatures ranged from 425° to 600°C .

Interdigital detectors were fabricated by depositing gold electrodes in the same manner as on the silicon samples. The contacts on the sputtered germanium were ohmic with linear I-V characteristics. One group of detectors (on higher resistivity films) had dark resistances of $13\text{ k}\Omega$ while a second group had dark resistances near $640\text{ }\Omega$. The responsivity of these detectors was measured using illumination with a chopped He-Ne laser and found to be 1.1 A/W and 0.1 A/W for the high and low resistivity germanium, respectively.

The response speed of the Ge-on-GaAs detectors was measured using the 70 psec diode laser pulses. As shown in Fig. 4 the pulse response was about 500 psec (FWHM), considerably faster than the photoconductive detectors on bulk silicon.

The low frequency response was also measured using an infrared He-Ne laser operating at a wavelength of $1.15\text{ }\mu\text{m}$. The responsivity increased slightly at the longer wavelength. Also, since the GaAs substrate is partially transparent at $1.15\text{ }\mu\text{m}$ the detector could be illuminated either from above the film surface or through the substrate. When illuminated through the GaAs, the responsivity was 20% of that observed for front face illumination. But these GaAs substrates (with no germanium film) had an optical transmission of only 20%. So we conclude that the germanium detectors were equally efficient in both geometries. This is an important consideration for future use of GaAs as a waveguide medium or for heterojunction diode photodetectors.

With the e-beam evaporated films the I-V characteristics indicated that the detectors' contacts were Schottky barriers, rather than ohmic. We have not yet evaluated these detectors in detail.

We will continue to investigate the use of evaporation for epitaxial film growth, including Si on GaAs using a Ge epilayer as an intermediary. Initial attempts at this have been made but more work is required to improve the substrate preparation and vacuum conditions before single crystal layers are possible.

3. THIN FILM OPTICAL WAVEGUIDES

The objective of this investigation was to develop techniques for producing low loss optical waveguides by rf sputtering and to fabricate passive waveguide channels. These should be capable of efficiently delivering optical signals to small area detectors or optoelectronic switching elements in an optical integrated circuit. The substrates were either thermally oxidized silicon wafers or microscope slides made from fused quartz or glass. Typical sputter deposition conditions were as follows. Four inch diameter targets were used and sputtering powers ranged from 40 to 400 watts. A mixed oxygen plus argon atmosphere was used in all cases, so that reactive sputtering maintained sufficient oxygen content in the growing film. Gas pressures ranged from 2 to 3.6 mTorr and O_2 content from 20% to 60%. Substrate temperatures ranged from (nominally) room temperature to 350°C.

The most useful technique for evaluating the optical properties of the sputtered films was to prism couple [10] a He-Ne laser beam into the waveguide. The waveguide attenuation was measured by collecting scattered light from different positions along the waveguide with an optical fiber. When the losses were relatively high, the observed length of the stripe of guided light could be used as an approximate measure of the losses using the "27 dB rule" [11]. When the waveguides were sufficiently thick to be multi-mode, the refractive index and thickness of the films could be determined from a measurement of the prism coupling angles [12].

Three different materials were studied for waveguide fabrication: GeO_2 , ZnO and a barium borosilicate glass (Corning no.

7059). These are discussed separately below.

i) Germanium Dioxide:

GeO_2 is a commonly used dopant for optical fibers and there has been recent interest both at McMaster [13] and elsewhere [14] in the use of GeO_2 or $\text{GeO}_2\text{:SiO}_2$ mixtures for thin film optical waveguides. Thin films were deposited by sputtering from a GeO_2 target on to unheated substrates using an $\text{Ar}:\text{O}_2$ ratio of 1:1 and a total gas pressure of 2 mTorr. It was found that the lowest optical losses were achieved using the lowest practical sputtering power. Therefore we generally operated at 40-50 watts which resulted in a growth rate of about .04 $\mu\text{m/hr}$. Using ten hour depositions the films were about .4 μm thick which meant they supported only the lowest TE and TM propagation modes. The measured propagation loss was typically a few dB/cm with the best results being below 1 dB/cm. In our earlier experiments, using a "home-made", pressed-powder target, the as-grown films had losses between 10 and 20 dB/cm but annealing for several hours at 250°C reduced this to < 1 dB/cm. Later experiments using a commercially obtained target resulted in approximately 1 dB/cm losses without any annealing, and only slight improvement after annealing.

This attenuation level is sufficiently low for most integrated optics applications and we had previously exploited the photorefractive effect in GeO_2 to fabricate narrowband waveguide filters [13]. However, the GeO_2 films are water soluble and this poses some difficulties. Unprotected films tend to degrade over a period of many weeks as moisture from the air is absorbed.

Also they are not well suited for the fabrication of narrow (several micron wide) channels which are essential for integration of waveguides with optical sources and detectors. We did experiment with a somewhat unconventional photolithographic process. Rather than etching away portions of the GeO_2 film with acid, we simply took advantage of the fact that when the photoresist was put in the developer, the developer itself removed not only the exposed photoresist but the GeO_2 film below it. Subsequently, when the unexposed photoresist was removed with acetone, channels of GeO_2 were left behind. This worked well for channels which were 100 microns wide but for narrower channels it was too difficult to control the etch rate precisely and avoid damaging the waveguides. It was decided that an alternative waveguide material should be used for integration with detector elements. However, in defense of GeO_2 , it should be pointed out that it has given us the lowest attenuation, so far, in a planar waveguide and that it may be possible to overcome some of the processing difficulties by covering the films with a SiO_2 encapsulation layer. This was done, using e-beam evaporation to deposit an approximately $0.1 \mu\text{m}$ thick film on top of the waveguide layer. Encapsulation improved the shelf life of the GeO_2 waveguide considerably but we have not yet investigated its effects on photolithographic processing.

ii) Zinc Oxide:

Zinc oxide is a large bandgap semiconductor which is transparent throughout the visible and near infrared and has a refractive index of 2.0. Sputtered films of ZnO are widely used, mostly for surface acoustic wave applications, but a number of

groups have also studied its use as an optical waveguide material [11,15]. In fact, one of the smallest attenuation figures ever reported for thin film waveguides was for laser annealed ZnO [16].

Sputtered ZnO films tend to grow in a filamented polycrystalline structure with the c axis normal to the substrate (even when the substrate is amorphous). This makes it an attractive material for active integrated optical devices in which surface acoustic waves are used to switch or modulate beams of light. But for passive devices crystallinity is not required and it can be detrimental if grain boundaries contribute significantly to optical scattering losses.

Reactive sputtering from both ZnO and Zn targets was used. The pure zinc target was preferred because with it there was no flaking of small particles from the target onto the substrate below. Also its higher thermal conductivity improved target cooling. Typically, sputtering was carried out with a total pressure of 3.6 mTorr and an oxygen content of 20-40%. The quality of the resulting waveguides depended very critically on the specific rf power and substrate temperature used, as shown in Fig. 5. The lowest attenuation (~ 9 dB/cm) was obtained with a combination of 100 W and 278°C or 200 W and 287°C . But at any given sputtering power, rather small deviations from the optimum temperature resulted in much greater optical losses.

These high losses are attributed largely to surface scattering, rather than bulk absorption. This was inferred from the rate at which the losses increased as a function of waveguide

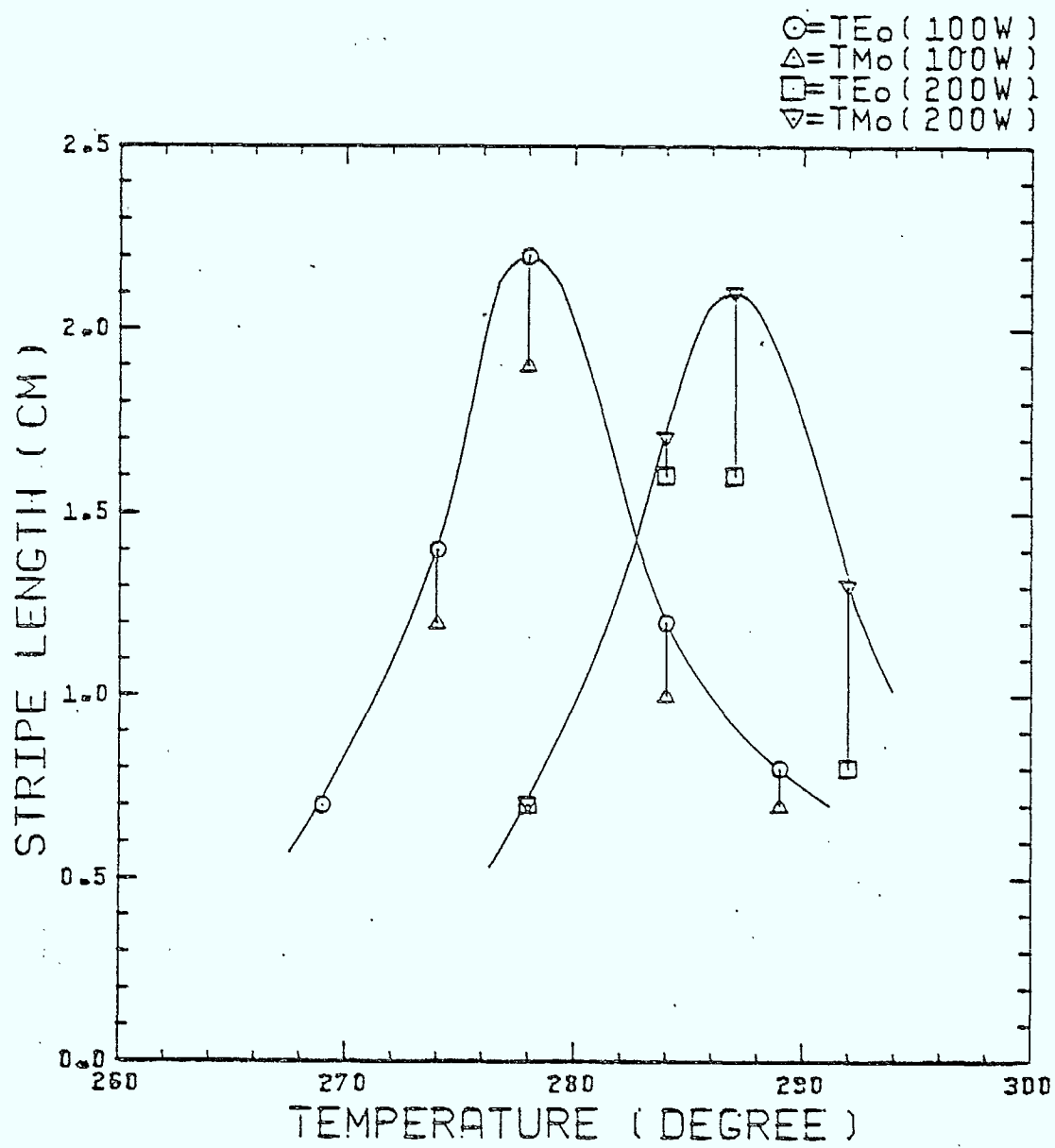


Figure 5

mode number. Converting mode number and thickness into an effective number of "bounces per micron" and then extrapolating back to zero bounces gave a value of less than 1 dB/cm for the bulk losses, similar to observations by other groups [11,15]. Scanning electron microscope (SEM) observation of films (see Fig. 6) showed clearly the filamented, polycrystalline nature of the growth and a very high degree of top surface roughness. Mechanical polishing, using a 0.03 μm sized abrasive in deionized water, was found to reduce the attenuation of lossy waveguides from 50 to 20 dB/cm which also indicates that surface scattering is the dominant loss mechanism.

In comparing our results to those reported in the literature, the rather high loss ($\sim 9\text{dB/cm}$) for the as-grown films appears to be typical. The extremely low losses that have been reported come about only after various annealing procedures. We investigated both CO_2 laser annealing and annealing using a quartz lamp "heat-pulse" furnace. For the former we used a 20 watt, continuous CO_2 laser operating at a wavelength of 9.2 μm . The laser was focussed to give an intensity of approximately 1 kW/cm^2 and the beam was raster scanned across the ZnO film on an oxidized silicon substrate. (The laser would crack glass or quartz substrates at this intensity). Unfortunately, no significant reduction in waveguide losses was achieved and higher laser intensities were found to damage the substrate. Dutta et al. [16] report that intensity levels of 10^5 watts/ cm^2 at a wavelength of 10.6 μm are required and the system we were using could not quite provide this. But laser annealing has been shown to be very useful and is obviously an area where more effort

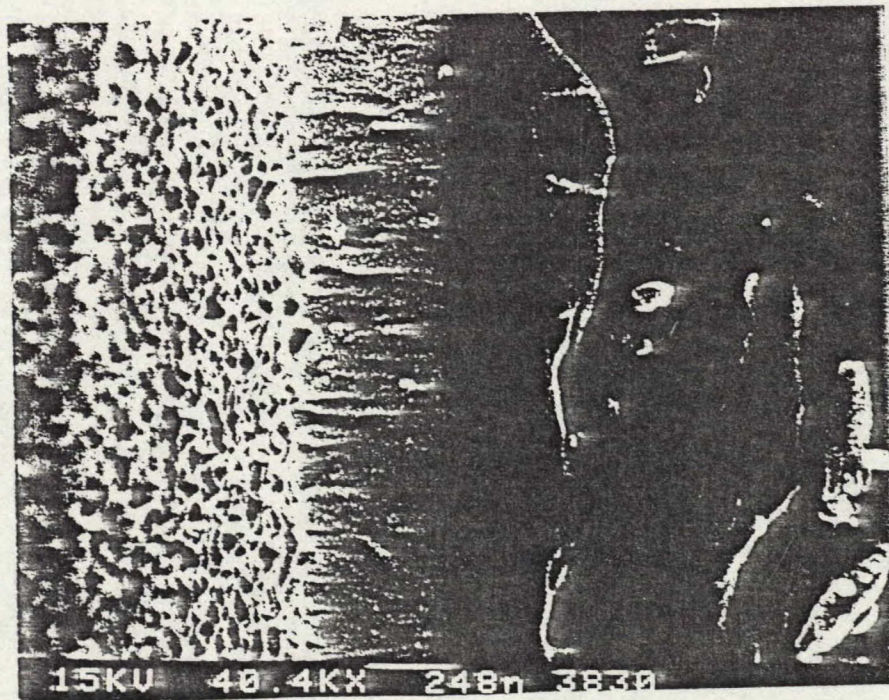
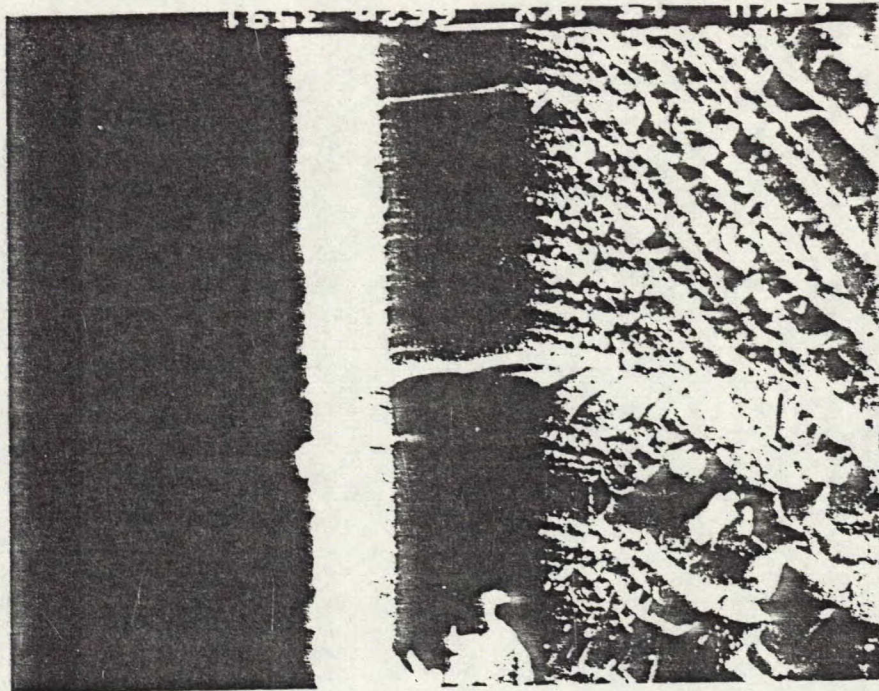


Figure 6

should be placed.

For the heat-pulse furnace annealing, the samples were heated to 1250°C in a few seconds, held there for 1 second and then rapidly cooled. This had a dramatic effect on the degree of crystalline perfection as indicated by the intensity and widths of the (002) x-ray diffractometer peak, and crystalline perfection, in turn, has been associated with reduced optical loss [11]. The (002) peak showed thirteen times increase in height and a narrowing from a linewidth of 0.54° to 0.286° (FWHM). However, SEM photographs showed some cracking due to the thermal shock and no reduction in waveguide losses were observed. CO_2 laser annealing is more promising than heat pulse annealing because it deposits heat primarily in the film and not in the substrate, which is transparent at the laser wavelengths.

As expected, the ZnO films proved to be suitable for narrow channel fabrication using standard photolithography. A test mask consisting of a series of straight lines having widths 12, 25 and $50\text{ }\mu\text{m}$ was used and the ZnO was etched with a dilute HCl solution. Laser light could be efficiently coupled into the channels and their optical quality was not harmed by the photolithographic processing.

In summary, the main difficulties we experienced with ZnO were that the optical loss was always several dB/cm, or more. Also the optical quality depends so critically on the precise sputtering conditions that good results are difficult to obtain on a routine and repeatable basis. We therefore turned to a third material which proved far better in this respect.

iii) Corning 7059 Glass:

Corning 7059 glass is a barium borosilicate glass with a refractive index of 1.53. It is standard glass product, readily available in large sheets, and is often used as a substrate material. It is certainly not the only type of glass that could be sputtered to make thin film waveguides but it is probably the most popular [2,12]. A four inch diameter, one mm thick disk of this material was epoxied to an aluminum backing plate to make a sputtering target. Typically 200 W of sputtering power was used with unheated substrates and an $O_2:Ar$ ratio of 1:4. The sputtering rate was found to be quite low. It required 7-8 hours to grow a $0.35 \mu m$ thick film. Other researchers [17] have noted that films sputtered from 7059 glass targets can have refractive index values ranging from 1.53 to 1.59, depending on sputtering power. Our films had an index value consistently in the range of $1.59 \pm .01$.

In comparison to ZnO , the big advantage of the glass waveguides is that the attenuation levels were lower and the film quality much more consistent from run to run because a much wider range of sputtering conditions was acceptable. The losses of as-grown film were usually 3-5 dB/cm and this was easily reduced to below 2 dB/cm by the spin-on application of an SiO_2 film. Although we would like to reduce these losses still further, they are sufficiently low to be adequate for experiments involving integration of waveguide channels with detectors. Consequently, only the glass waveguides were used for that work.

The integration experiment required waveguide channels with widths of $8 \mu m$. These were obtained using standard photolitho-

graphic techniques and buffered HF acid as an etchant (see appendix). The acid concentration and temperature were chosen to give sharp channel edges with a minimum of taper due to lateral etching [18]. It was required to carefully control the etching time in order that the unwanted glass be completely removed while not over-etching the channels themselves. If this were to occur, undercutting and photoresist lift-off would cause damage to the channels due to exposure to the acid. Once the proper etchant parameters were established, good optical quality channels could be consistently produced.

Fig. 7 shows two SEM photographs of the same 8 μm wide channel. The upper view shows a length of channel at a magnification of 1500X and demonstrates the edge quality over $\sim 50 \mu\text{m}$ length. Below is a view of the cleaved edge at a higher magnification (10,000X). Here the fractured end of the channel is seen with the thermally grown SiO_2 underlying the waveguide.

Besides the straight channels for integrated detectors, Y-branch channels (with branching angles from 3.5° - 7.5°) have also been produced. These channels divided the optical power in the correct 50:50 ratio (to within a measurement accuracy of several percent) and they showed no measureable excess optical losses above that associated with straight channel sections.

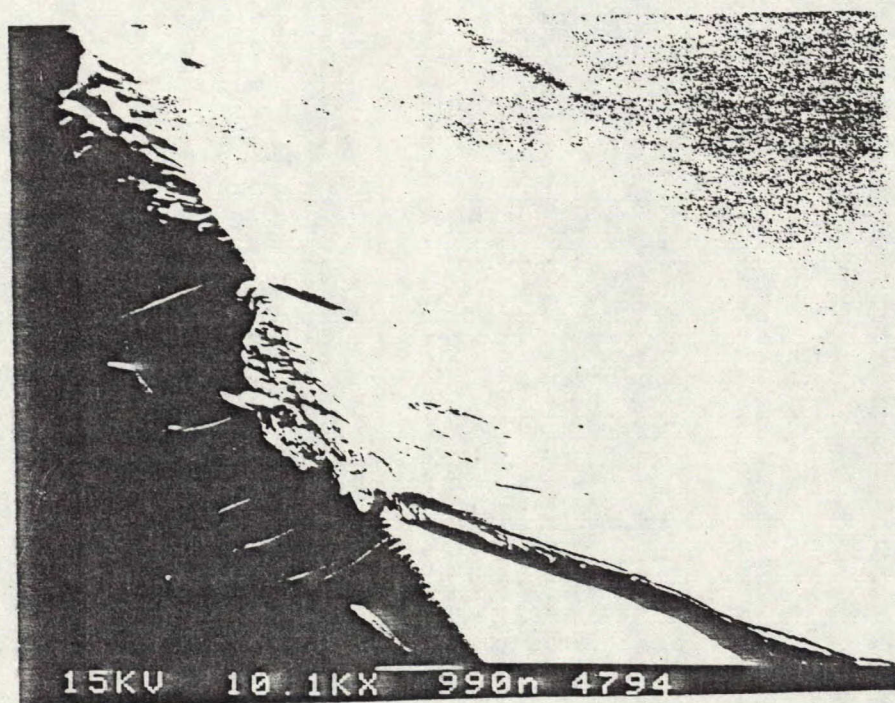
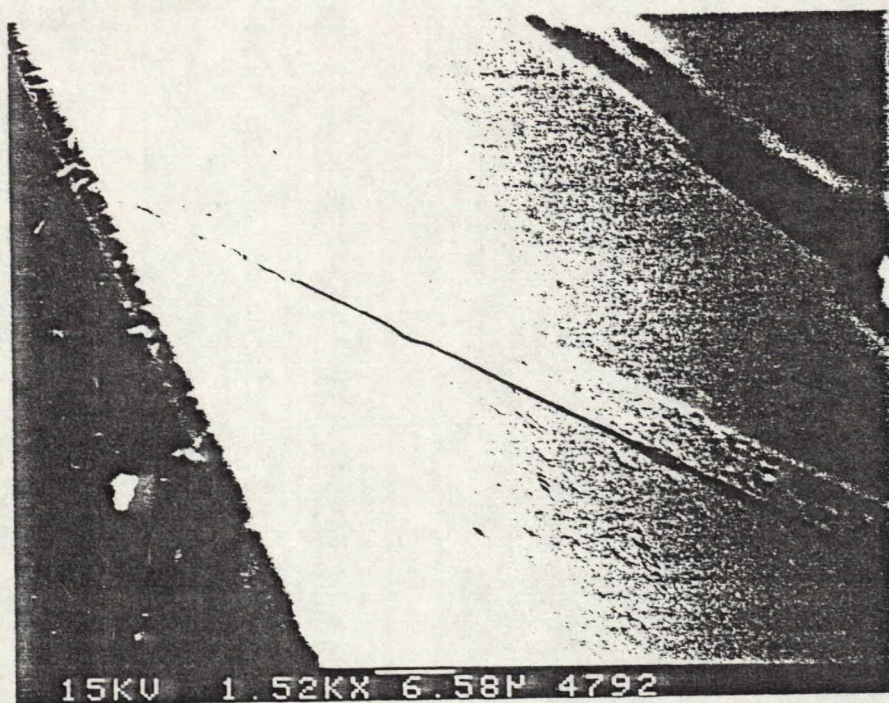


Figure 7

4. INTEGRATED OPTICAL DETECTORS

One of the most fundamental components of future monolithically integrated optical systems will be a photodetector which is illuminated through a waveguide channel, co-fabricated on the same substrate as the detector itself. Numerous different approaches to this problem have recently been reported [19,20]. We have designed a detector which is a modified version of the photoconductor described in section 2, incorporating a narrow glass waveguide channel which delivers light precisely to the very small active area between the metal electrodes.

Each detector is simply a pair of long metal electrodes, separated by a 12 μm gap. A linear array of 40 such detectors was fabricated using mask #2, as illustrated in the lower portion of Fig. 8. A series of long electrodes were connected in common, with shorter electrodes in between (at the top in the illustration). The interelectrode gap was too narrow to be visible in Fig. 8. Mask #3, shown on the upper portion of Fig. 8, was used to make a series of waveguide channels such that each channel fed light into one or two elements of the detector array.

Fabrication of these devices began with the thermal oxidation of a 10 ohm-cm, p-type, silicon wafer. The approximately 1 μm thick SiO_2 layer formed was required as an intermediate buffer layer for the thin film waveguides. Mask #1 was then used to cut holes through the silicon with a buffered HF acid etch (see appendix). These openings through to the silicon correspond to the 40 detectors in the array shown in Fig. 8. A detailed view of a single element of mask #1 is given in the upper portion of Fig. 9. Each of the elements is 200 μm wide and 500 μm long. A

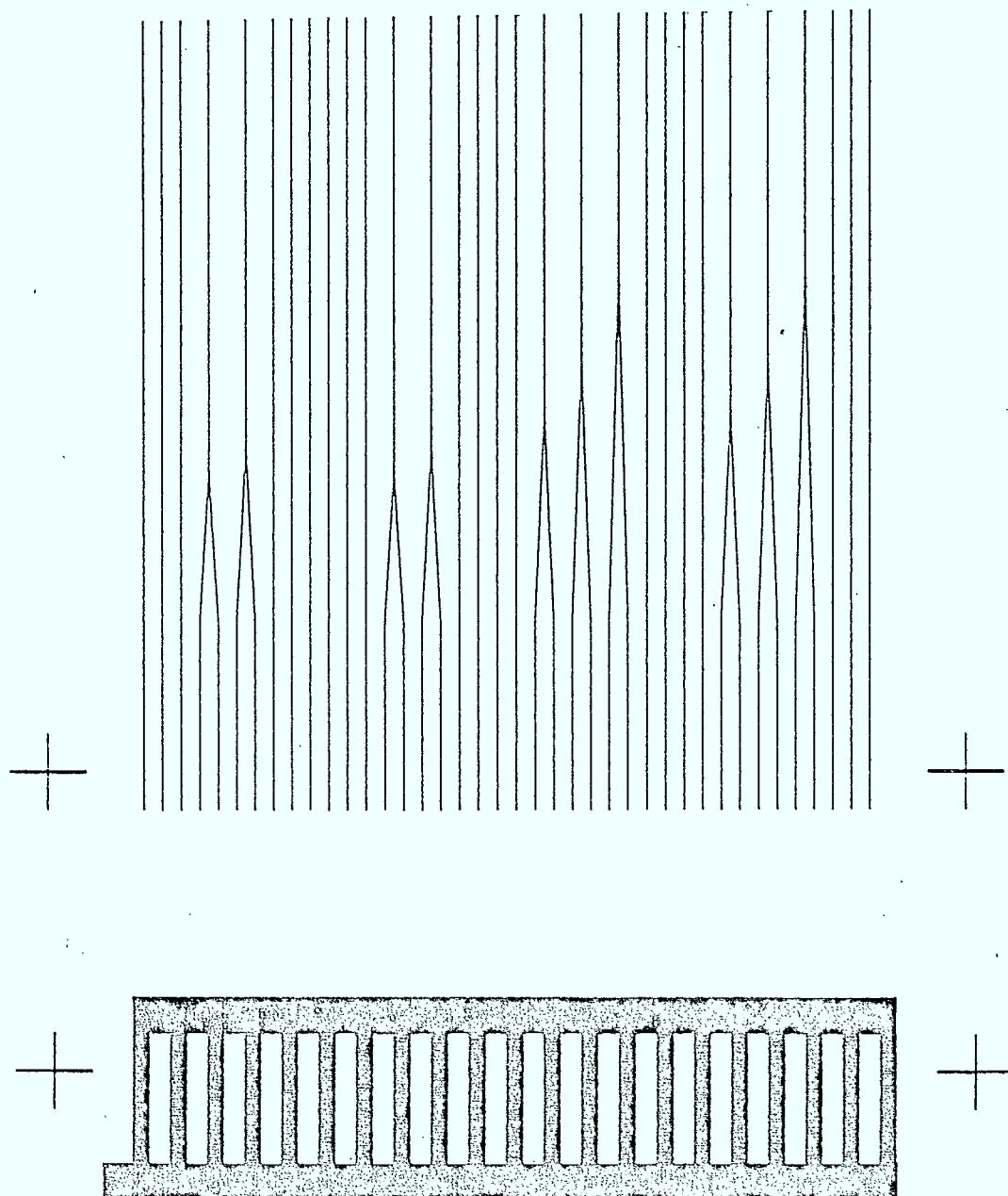
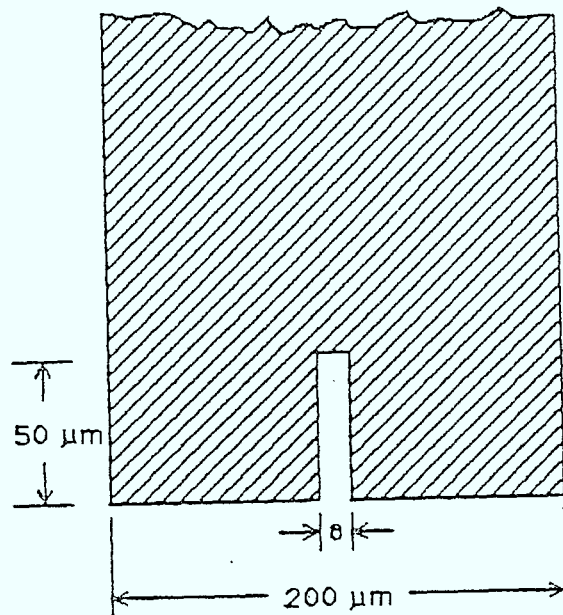
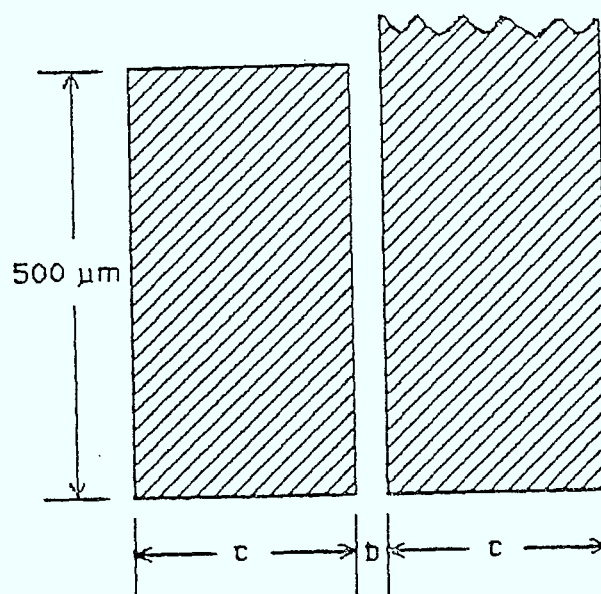


Figure 8



$$a = 10\ \mu\text{m}$$



$$b = 12\ \mu\text{m}$$

$$c = 250\ \mu\text{m}$$

Figure 9

small central strip of SiO_2 ($10\text{ }\mu\text{m}$ wide and $50\text{ }\mu\text{m}$ long) remains at the front of the opening, this corresponding to the position of the overlying waveguide channel. The purpose of the strip was to ensure that the optical radiation travelling in the waveguide will be well inside the detector region before any light is absorbed into the silicon.

The next step required that the wafer be metallized by the thermal evaporation of gold to a thickness of approximately $0.1\text{ }\mu\text{m}$. The detector electrodes were then defined by masking (with mask #2 aligned with respect to the holes and strips in the SiO_2) and etching with potassium iodide (see appendix). The dimensions for the electrode contacts are shown on a single element in the lower portion of Fig. 9. Here the separation between the contacts is $12\text{ }\mu\text{m}$ for the $8\text{ }\mu\text{m}$ channels. This larger size is intended for alignment tolerances throughout the photolithographic processing.

Following this the substrates were cleaned and then introduced into the rf sputtering system where the thin glass films were formed. The next step was to mask (mask #3, upper portion of Fig. 8) and etch the waveguide channels, as outlined in the previous section. These channels were aligned along the SiO_2 strip between each of the gold detector elements. Finally, individual detectors were contacted with fine gold wire using an ultrasonic bonder.

The responsivity of these detectors was measured first by illuminating them with a chopped He-Ne beam focussed directly onto the active area. Dividing a typical observed photocurrent

of 0.14 mA by the received optical power of .086 mW (4.9 mW/mm^2 in the focussed beam x a detector active area of .0175 mm^2) gave a responsivity of 1.6 amps/watt. This is quite consistent with the observed responsivity of the interdigitated photoconductive detectors made using silicon of the same resistivity.

The first attempt to measure the response to light coupled into the detector via a waveguide channel was made by prism coupling the chopped He-Ne laser into the appropriate channel. However, this did not constitute a valid measurement because there was insufficient discrimination between light that was absorbed in the detector's small "active area" and light absorbed elsewhere on the silicon surface. The 10 μm wide gap region between the electrodes is far more sensitive than the surrounding silicon, but the prism coupling was far from optimized and the waveguide channel far from lossless. So there was a great deal more light leaked into the semiconductor by refraction and scattering at the base of the prism and along the length of the channel (5-10 mm) than was actually delivered to the detector element. Thus for DC or very low frequency signals the diffusion of carriers generated far from the interelectrode region could actually give a larger signal than that from the light absorbed in the high field "active area".

To investigate this effect further the chopped He-Ne laser was again focussed directly onto the detector surface (spot diameter of 0.4 mm) and the relative photocurrent recorded as the spot was moved across the silicon wafer surface, away from the detector. The results are shown in Fig. 10. The response falls drastically as the spot moves off the detector but a non-zero

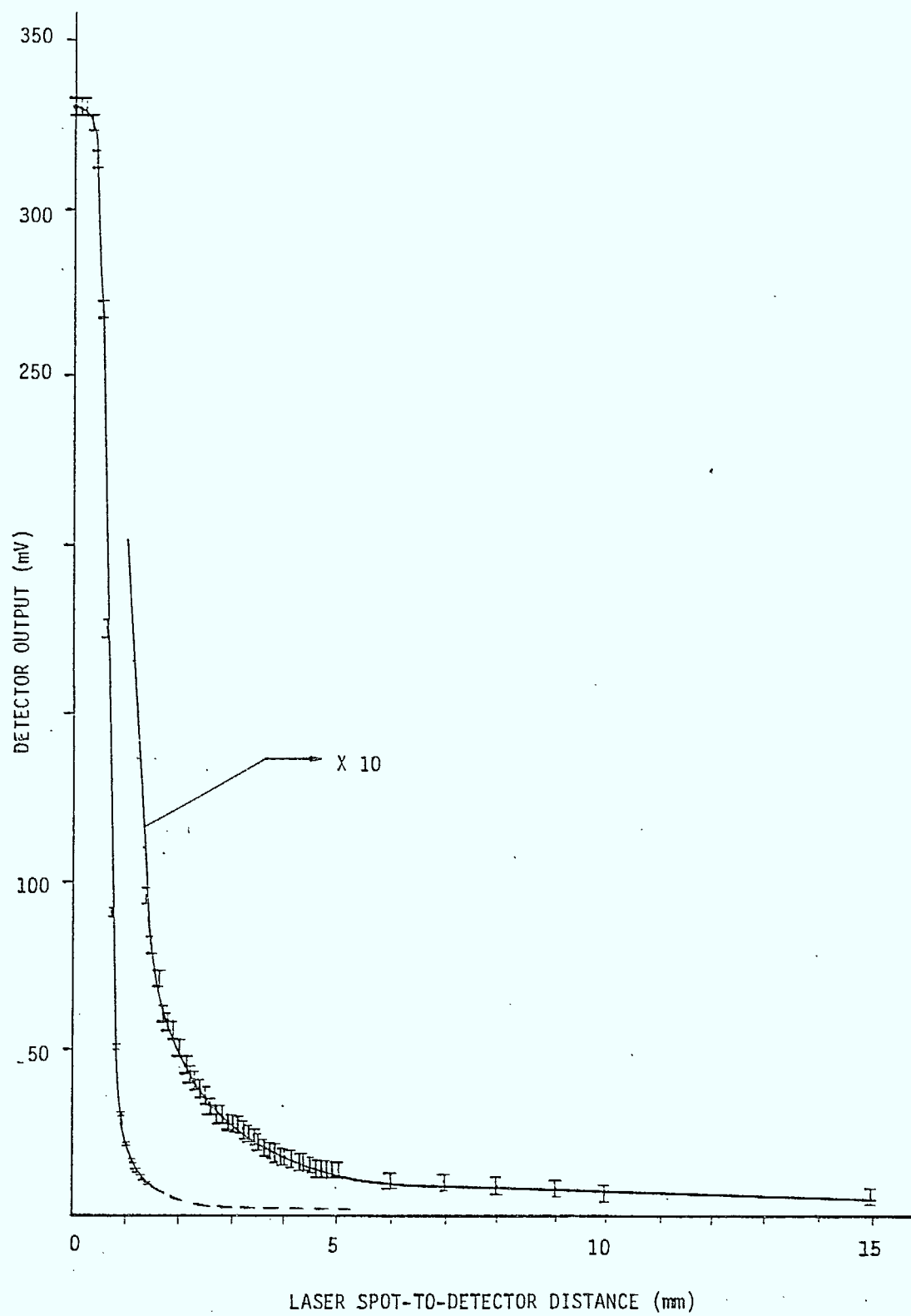


Figure 10

component due to long range carrier diffusion remains, even up to a distance of 15 mm. This contribution was relatively small. (We confirmed that it was too small to significantly affect the responsivity measurements made by direct illumination of the detectors by repeating the measurements at several different beam diameters and obtaining consistent results). But it did mean that low frequency responsivity measurements of the integrated detectors were unreliable.

For 10 ohm-cm silicon the diffusion constant is such that the observed diffusion decay length of a few mm (see Fig. 10) corresponds to a decay time on the order of a millisecond. Thus the responsivity at high frequencies will have a negligible contribution due to long range diffusion. Even with the mechanical chopper the long range response was demonstrably slow. When the rise time of the light pulse was 16 μ sec the rise and fall times of the detector response went from 16 to 40 to 80 μ sec for illumination on the detector, 1 mm away and 15 mm away, respectively.

To isolate the high frequency responsivity, an rf modulation was placed on the He-Ne laser beam. The component of the photocurrent at the modulation frequency was then measured either by direct observation of the detector output on an oscilloscope or by the use of an rf spectrum analyser. The laser that was used could be modulated at frequencies up to 1 MHz with a modulation depth of about 5 percent by supplying a 1.5 Volt (peak to peak) control signal to the power supply. With a modulation frequency below 10 kHz a significant photocurrent could still be generated

when the laser spot was focussed on the silicon surface several mm from the detector. But at 50 kHz it was reduced by almost a factor of ten and at 1 MHz it was totally suppressed. However, when the light was focussed on the area between the detector electrodes, where the photoresponse is very fast, the responsivity at 1 MHz was the same as that measured using the mechanical chopper. Thus, we were confident that by modulating at 1 MHz we could deliver light to the detector through a waveguide channel and measure the response only to light absorbed in the high field, active region.

The efficiency with which light was delivered to the detectors by the waveguide channels could be estimated by measuring the induced photocurrent and converting that to a received optical power (using the value of responsivity determined by the surface illumination). The efficiency is the received optical power divided by the power in the waveguide channel. Unfortunately, the latter was only approximately known since we did not have strict control over the efficiency of coupling the laser beam into the waveguide channel.

Initially, prism coupling was used. It is a very convenient method and required no special preparation of the waveguides. For planar waveguides this method can be very efficient, up to 90% [10]. But that requires careful tapering of the laser beam profile and can be very tedious. We did not make a serious effort to maximize coupling efficiency into planar waveguides and for routine measurements our efficiency was low, probably less than ten percent. When prism coupling is used with channel waveguides the efficiency is reduced still further because the

focussed laser beam, as it hits the base of the prism, is wider than the waveguide channel and most of the light misses the channel. Although the prism coupling efficiency was low, it was sufficient for most of the optical measurements made.

In the main experiment that was used to evaluate the integrated detectors, the He-Ne laser beam, modulated at 1 MHz, was coupled into a waveguide channel approximately 5 mm away from the detector element itself. The detector was connected in series with an external resistor ($50\text{--}1000\ \Omega$) and a bias voltage of from 2 to 10 volts applied across the series combination. The 1 MHz signal across the resistor was then monitored, either on an oscilloscope or by means of a spectrum analyser.

When prism coupling was used the results were as follows. The observed photocurrent had a 1 MHz modulation amplitude of 0.2 μamp (peak to peak). Using the responsivity value of 1.8 amps/watt (as determined by surface illumination measurements) this implies that the detected optical power was only 0.11 μW , as compared to 40 μW arriving at the prism coupler (4% modulation on a 1 mW beam). Thus the overall efficiency of delivering light to the detector was only 0.3%.

It was clear that prism coupling into the narrow channels was very inefficient and a major reason for the low overall efficiency. We therefore replaced this with "end-fire" coupling. In this case a reasonably flat end of a channel was exposed by scribing and breaking the wafer. Then a microscope objective was used to focus the input beam onto that end surface. Fig. 7 shows an SEM photograph of one such end. The surface is quite irregu-

lar but in spite of that, when a clean break is made across an entire row of 40 channels, it is possible to end-fire couple into almost all of them. The coupling efficiencies were obviously superior to prism coupling since the intensity of light seen in the waveguide channel was clearly greater. Attempts were made to improve the coupling by polishing the end faces but this was unsuccessful. It may be that using (100) oriented silicon wafers rather than (111), as was used throughout this work, would make it easier to prepare flatter end faces. With a (100) wafer the waveguides could be made perpendicular to the crystal's natural cleavage planes.

For our measured focal spot diameter of several μm and a typical waveguide thickness of $0.35 \mu\text{m}$ one could only expect an end fire coupling efficiency of about ten percent, even if the end faces were perfectly smooth. In practice it will be even less. To estimate the actual efficiency we prepared a short substrate on which a series of 4 mm long channels had "clean break" surfaces at both ends. Laser light was end-fire coupled into one end of a channel and collected at the other end by butt coupling a multi-mode optical fiber. The ratio of output to input intensities was taken to be the end-fire coupling efficiency. A 100% collection efficiency at the output end was assumed but an attenuation of 50% along the channel was allowed for since, with these particular waveguides, there was a visible decrease in intensity over the channel length. The result was an estimate of 3 % for the highest observed coupling efficiency with 1 % being a more typical value.

When end-fire coupling was used to couple a 1 MHz modulated

He-Ne beam into the waveguide channel of an integrated photodetector the following results were obtained. The photocurrent had a modulation amplitude of $1.0 \mu\text{amp}$ (peak to peak) which implies a detected power of $0.59 \mu\text{watt}$, given the measured responsivity of 1.7 amp/watt . The laser beam power was 0.74 mW (measured after the microscope objective). The 7.7% depth of modulation therefore produced a $57 \mu\text{W}$ input modulation. Thus, the overall efficiency of delivering light to the detector was about 1.0%. This is improved somewhat over the prism-coupled case but is still quite small.

This efficiency is the product of three factors; the end-fire coupling efficiency, the transmission of the waveguide channel, and the efficiency of coupling from the waveguide into the detector. As discussed above the first of these must be less than ten percent, based strictly on geometrical considerations. Imperfect surface preparation almost certainly reduces it to only a few percent, as indicated by our independent coupling efficiency experiments. Also the transmission factor for the waveguide channels was estimated to be 0.7, or less. Thus, for the overall efficiency to be .01, as measured, we conclude that the waveguide-to-detector coupling is quite efficient, at least 20%, and probably much better.

It is this waveguide-to-detector efficiency which is of greatest interest for this work. The problems of coupling into the waveguide and reducing its attenuation are well understood and common to all integrated optics devices. Simply making the waveguides thicker would greatly improve the input coupling effi-

ciency. The major objective of this project was to determine if our relatively simple integrated detector design would be an effective way to deliver light from a waveguide to a detector. The results we have obtained are very encouraging.

5. CONCLUSIONS

We have fabricated both Schottky barrier photodiodes and photoconductive detectors by forming interdigital electrodes on silicon-on-sapphire (SOS), bulk silicon and germanium-on-gallium arsenide surfaces. The fastest observed response time was less than 30 psec, for the photodiodes on SOS. This high speed is due, in part, to the very low depletion capacitance which is possible using a semiconductor epilayer on an insulating substrate.

The main emphasis of the work, however, was on the photoconductive detectors. Picosecond response times are also possible with photoconductors and they have an added advantage for optoelectronic switching applications. There are no charge accumulation and depletion layers to slow down switching of the bias state. The photoconductive detectors which were made on high resistivity p-type silicon had responsivities above one amp/watt, indicating the presence of photoconductive gain. Their response times were 1-3 nsec, similar to the Schottky barrier photodiodes fabricated on the same material. The Ge-on-GaAs layers produced photoconductors with response times of 500 psec. This is still considerably slower than has been reported for similar devices fabricated on GaAs [6].

An integrated optical detector, consisting of a photoconductor coupled to a narrow channel optical waveguide, was designed and built. Standard silicon device fabrication technology was used, making this type of detector ideally suited for integration with silicon electronic circuitry. The detector responsivity was about 1.5 amps/watts, as in the case of the interdigital detec-

tors. The overall efficiency of coupling an external laser beam into the integrated detector was measured to be only about one percent. But the losses were dominated by inefficient initial coupling of the beam into the waveguide channel and by attenuation within the channel, both of which can be improved relatively easily. The most important parameter, as far as the design of the integrated detector is concerned, is the efficiency of coupling light from the waveguide channel into the detector element and this was very high.

The integrated optical detector is very promising for optoelectronic switching applications and for integrated optics, in general. Future work in this area should involve fabrication of arrays of detector elements to make a switching matrix and extension to III-V epilayer systems in order to achieve higher speeds.

APPENDIX

1. Cleaning Procedures:

- a. Preparation for thermal oxidation: the silicon wafers were immersed for 10 minutes each in a boiling solution of $\text{H}_2\text{SO}_4/\text{H}_2\text{O}_2$ (20% H_2O_2) and a boiling solution of $\text{HCl}/\text{H}_2\text{O}_2$ (20% H_2O_2). Following this the wafers were immersed for 5 minutes each in solutions of trichloroethylene (TCE), acetone, methanol and deionized water in an ultrasonic cleaner.
- b. Preparation for gold and sputtering depositions: an ultrasonic cleaning for 5 minutes each in TCE, acetone, methanol and deionized water. This was followed by a 20-30 second etch in a dilute HF solution (~ 1% HF).
- c. Preparation prior to photoresist application: an ultrasonic cleaning for 5 minutes each in TCE, acetone, methanol and deionized water. When preparing for etching of either thermally grown SiO_2 or sputtered glass, a 1-2 hour dehydration bake at 150°C preceded the application of photoresist.

2. Etching Procedures

- a. Gold etch: a solution of $\text{KI}/\text{I}_2/\text{H}_2\text{O}$ (40 gm/10gm/400gm) was used giving an etch rate of ~ 50 Å/sec.
- b. Aluminum etch: a 1% HF solution was used with an etch rate of ~ 10 Å/sec.
- c. Silicon dioxide etch: a buffered HF solution was used at various concentrations and temperatures to give the desired etching results. Typically a solution of

HF/NH₄F with a 1:30 ratio at a temperature of 65° C gave etch rates of ~ 100 Å/sec. (HF is a 49% solution and NH₄F is a 40% solution by weight).

- d. Sputtered glass etch: a buffered HF/NH₄F solution was used at a concentration of 1:10 and a temperature of ~ 25° C to give etch rates of ~ 200 Å/sec.

REFERENCES

- [1] C.W. Slayman and L. Figueroa, "Frequency and pulse response of a novel high speed interdigital surface photoconductor (IDPC)," IEEE Electron Devices Lett., **EDL-2**, 112-114 (1981).
- [2] J.C. Gammel and J.M. Ballantyne, "An integrated photoconductive detector and waveguide structure," Appl. Phys. Lett., **36**, 149-151 (1980).
- [3] R.J. Seymour and B.K. Garside, "Ultrafast silicon interdigital photodiodes for ultraviolet applications," Can. J. Phys., **63**, 707-711 (1985).
- [4] R.J. Seymour, B.K. Garside and R.E. Park, "Ultrafast surface barrier photodetectors," SPIE International Symposium on Optical and Optoelectronic Applied Sciences and Engineering, Quebec City, Canada, June 1986, Paper 663-06.
- [5] S. Selberherr, Analysis and Simulation of Semiconductor Devices, Springer-Verlag, Wien, New York, 1984.
- [6] R.I. MacDonald and D.K. Lam, "Optoelectronic switch matrices: recent developments," Optical Engineering, **24**, 220-224 (1985).
- [7] K.C. Cadien and J.E. Greene, "Crystal growth and controlled doping of epitaxial Ge films on (100) GaAs by sputter deposition," J. Crystal Growth, **61**, 15-22 (1983).
- [8] C.J. Palmstrøm and G.J. Galvin, "Solid phase epitaxy of deposited amorphous Ge on GaAs," Appl. Phys. Lett., **47**, 815-817 (1985).
- [9] K.B. Sundaram and B.K. Garside, "Controlled doping of rf sputtered germanium films," Appl. Phys. A, **34**, 117-121 (1984).
- [10] Z-Y. Yin and B.K. Garside, "New configurations for high-efficiency prism couplers with application to GeO₂ optical waveguides," Appl. Opt., **22**, 1023-1028 (1983).
- [11] F.S. Hickernell, "Low loss zinc oxide optical waveguides on amorphous substrates," Digest of the Topical Meeting on Integrated and Guided Wave Optics, W36-1, (1980).

- [12] T. Tamir, Integrated Optics, Springer-Verlag, Berlin, Heidelberg, New York, 1979.
- [13] Z-Y. Yin, P.E. Jessop and B.K. Garside, "Photoinduced grating filters in GeO_2 thin-film waveguides," *Appl. Opt.*, **22**, 4088-4092 (1983).
- [14] A.S. Huang, Y. Arie, C.C. Neil and J.M. Hammer, "Study of refractive index of $\text{GeO}_2\text{:SiO}_2$ mixtures using deposited-thin-film optical waveguides," *Appl. Opt.*, **24**, 4404-4407 (1985).
- [15] M. Bertolotti, A. Ferrari, A. Jaskow, A. Palma and E. Verona, "Laser annealing of ZnO thin films," *J. Appl. Phys.*, **56**, 2943-2947 (1984).
- [16] S. Dutta, H.E. Jackson, J.T. Boyd, F.S. Hickernell and R.L. Davis, "Scattering loss reduction in ZnO optical waveguides by laser annealing," *Appl. Phys. Lett.*, **39**, 206-208 (1981).
- [17] C.W. Pitt, F.R. Gfeller and R.J. Stevens, "R.F. sputtered thin films for integrated optical components," *Thin Solid Films*, **26**, 25-51 (1975).
- [18] G.I. Parisi, S.E. Haszko and G.A. Rozgonyi, "Tapered windows in SiO_2 : The effect of $\text{NH}_4\text{F}\text{:HF}$ dilution and etching temperature," *J. Electrochem. Soc.: Solid-state science and technology*, **124**, 917-921 (1977).
- [19] R.F. Carson, T.E. Batchman and M.L. McWright, "High-efficiency coupling into planar waveguide thin-film photodetectors," Paper FA3, Conference for Lasers and Electro-Optics, Baltimore, May, 1985.
- [20] R. Trommer, "Monolithic InGaAs photodiode array illuminated through an integrated waveguide," *Electronics Letters*, **21**, 382-383 (1985).

JESSOP, P. E.

--High speed switching...

P

91

C654

J47

1986

DATE DUE

DATE DE RETOUR

[illegible]

LOWE-MARTIN No. 1137

CRC LIBRARY/BIBLIOTHEQUE CRC
P91.C654 J47 1986

INDUSTRY CANADA / INDUSTRIE CANADA



208222

